

Analysis of relative wavelength response characterization and its effects on scanned-WMS gas sensing

Dao Zheng(郑道), Zhi-Min Peng(彭志敏), Yan-Jun Ding(丁艳军), and Yan-Jun Du(杜艳君)
Citation: Chin. Phys. B, 2021, 30 (**4**): 044210. DOI: 10.1088/1674-1056/abdb1c
Journal homepage: http://cpb.iphy.ac.cn; http://iopscience.iop.org/cpb

What follows is a list of articles you may be interested in

Laser absorption spectroscopy for high temperature H_2O time-history measurement at 2.55 μm during oxidation of hydrogen

Yu-Dan Gou(苟于单), De-Xiang Zhang(张德翔), Yi-Jun Wang(王易君), Chang-Hua Zhang(张昌华), Ping Li(李萍), Xiang-Yuan Li(李象远)
Chin. Phys. B, 2018, 27 (**7**): 074213. DOI: 10.1088/1674-1056/27/7/074213

Self-calibration wavelength modulation spectroscopy for acetylene detection based on tunable diode laser absorption spectroscopy

Qin-Bin Huang(黄秦斌), Xue-Mei Xu(许雪梅), Chen-Jing Li(李晨静), Yi-Peng Ding(丁一鹏), Can Cao(曹粲), Lin-Zi Yin(尹林子), Jia-Feng Ding(丁家峰)
Chin. Phys. B, 2016, 25 (**11**): 114202. DOI: 10.1088/1674-1056/25/11/114202

Analysis of algebraic reconstruction technique for accurate imaging of gas temperature and concentration based on tunable diode laser absorption spectroscopy

Hui-Hui Xia(夏晖晖), Rui-Feng Kan(阚瑞峰), Jian-Guo Liu(刘建国), Zhen-Yu Xu(许振宇), Ya-Bai He(何亚柏)
Chin. Phys. B, 2016, 25 (**6**): 064205. DOI: 10.1088/1674-1056/25/6/064205

Sensitive absorption measurements of hydrogen sulfide at 1.578 μm using wavelength modulation spectroscopy

Xia Hua, Dong Feng-Zhong, Wu Bian, Zhang Zhi-Rong, Pang Tao, Sun Peng-Shuai, Cui Xiao-Juan, Han Luo, Wang Yu
Chin. Phys. B, 2015, 24 (**3**): 034204. DOI: 10.1088/1674-1056/24/3/034204

Dynamic thermal modeling and parameter identification for monolithic laser diode module

Li Jin-Yi, Du Zhen-Hui, Ma Yi-Wen, Xu Ke-Xin
Chin. Phys. B, 2013, 22 (**3**): 034203. DOI: 10.1088/1674-1056/22/3/034203

Analysis of relative wavelength response characterization and its effects on scanned-WMS gas sensing*

Dao Zheng(郑道), Zhi-Min Peng(彭志敏), Yan-Jun Ding(丁艳军), and Yan-Jun Du(杜艳君)†

State Key Laboratory of Power Systems, Department of Energy and Power Engineering, Tsinghua University, Beijing 100084, *China*

(Received 17 December 2020; revised manuscript received 10 January 2021; accepted manuscript online 13 January 2021)

Our recently proposed three-step method showed the promising potential to improve the accuracy of relative wavelength response (RWR) characterization in the wavelength-modulation spectroscopy (WMS) over the commonly used summation method. A detailed comparison of the three-step method and the summation method, for the wavelength-scanned WMS gas-sensing, was performed with different laser parameters (modulation indexes and scan indexes) and gas properties (pressures and concentrations). Simulation results show that the accuracy of the predicted gas parameters is strongly limited by the RWR characterization with large modulation index and high gas pressure conditions. Both fitting residuals of RWR and errors of predicted gas parameters from the recently proposed three-step method are nearly 2 orders of magnitude smaller than those from the summation method. In addition, the three-step method is further improved by introducing a coupling term for the 2nd harmonic amplitude. Experiments with CO_2 absorption transition at 6976.2026 cm^{-1} were conducted and validated the simulation analysis. The modified-three-step method presents an improved accuracy in RWR description with at least 5% smaller fitting residual for all conditions compared with the three-step method, although the deviation of the deduced CO_2 concentrations between these two methods does not exceed 0.2%.

Keywords: tunable diode laser absorption spectroscopy, relative wavelength response characterization, scanned-wavelength-modulation spectroscopy (WMS)

PACS: 42.55.Px, 42.62.–b, 42.62.Fi **DOI:** 10.1088/1674-1056/abdb1c

1. Introduction

High detection-sensitivity and selectivity, a low detection-limit, fast response, and the non-invasive characteristic make tunable diode-laser absorption spectroscopy (TDLAS) a widely used technology for gas monitoring,[1–3] spectroscopy-parameter measurements,[4–7] and combustion diagnostics.[8–11] Direct absorption spectroscopy (DAS) and wavelength modulation spectroscopy (WMS) are the main techniques used in TDLAS measurements at laboratories and in practical measurement applications. Although frequency modulation spectroscopy (FMS) can provide more accurate detection,[12] this technique is not widely used due to its high demands with respect to equipment quality and system complexity.

The detection sensitivity of DAS is typically 10^{-3}, mainly because of the low-frequency noise coming from the detection equipment ($1/f$ noise). DAS represents, however, still the most common approach due to its simplicity and robustness. For researchers, the biggest advantage of DAS is the ability to obtain absorbance directly, which provides much information about gas properties and spectroscopy parameters.[13–16] The premise and basis of DAS are characterizing relative wavelength response (RWR) accurately since the absorbance is wavelength dependent. For WMS, the detection sensitivity can be effectively improved by modulation and demodulation processes, which shifts the detection frequency into the kHz range and makes a detection sensitivity of 10^{-6} achievable.[17] One straight-forward way to measure gas properties using the WMS technique is to obtain the amplitude of certain harmonics, such as the second harmonic.[18] This can be done by demodulating the sampled signal and establishing a relationship between the amplitudes and gas properties. However, this method is heavily affected by laser power and electronic noise, i.e., background noise. Li *et al.*[19] proposed a calibration-free WMS (CF-WMS) method, which uses the first harmonic normalized second harmonic ($2f/1f$). This approach provides a good solution to suppress the background noise effect that occurs in the original WMS measurement. Although it is hard to determine the absorbance directly for WMS, the extracted harmonic is evidence for both absorbance and wavelength dependency. Therefore, accurate RWR characterization is also necessary to achieve high-precision measurements in WMS.

A precise description of the RWR is extremely important because absorbance and harmonics are both wavelength dependent. However, it is not that easy to obtain, especially in WMS. With the combination of scan and modulation, the main difficulty for the RWR characterization in WMS is locating and labelling the tremendous amount of etalon peaks. Many researchers have contributed to finding simpler and more efficient ways to determine the RWR in WMS to improve the

*Project supported by the National Natural Science Foundation of China (Grant Nos. 51906120 and 11972213), China Postdoctoral Science Foundation (Grant Nos. 2018M640125 and 2019T120088), and the National Basic Research Program of China (Grant No. 2016YFC0201104).

†Corresponding author. E-mail: duyanjun13@gmail.com

© 2021 Chinese Physical Society and IOP Publishing Ltd

measurement accuracy. The conventional method to characterize RWR in WMS is a summation of scan relative wavelength response in frequency f_s and modulation relative wavelength response in frequency f_m without any consideration about the physical properties of lasers,[19–21] which results in a relatively large deviation from the real RWR. In fact, the wavelength modulation index is related to the bias current even though the amplitude of the modulation current is fixed. Kluczynski found that the wavelength modulation index varies significantly from the beginning to the end of the sweep current.[22] Many researchers proposed to use the first derivative of the RWR with a scan frequency f_s to describe the changing wavelength-modulation index.[23,24] In addition, Ma *et al.* have found a method to determine the RWR.[25,26] They have not only considered the linear time-dependent amplitude of the first modulation term but also the constant amplitude of the second modulation term, and this reduced the final scanned-WMS-$2f/1f$ fitting residuals significantly. Furthermore, Ma *et al.* proposed a method to pre-determine the RWR, which is based on a second-order polynomial description of the RWR for the ramp-scan current. However, all these methods are based on the ramp current scan assumption and are available for the ramp scan current only, which limits its application range. With higher time-resolution, a sinusoidal-scanned WMS is more suitable for WMS detection, especially for combustion and some fast variation situations.[10,27–29] Du proposed a method, the 'three-step method', which can be used in sinusoidal-scanned or ramp-scanned WMS, with lower fitting residuals.[30] The modulation processes can be considered as modulation with changing bias current over a scan period, which can be described by the coupling terms as stated in Ref. [30]. This method can lower the fitting standard deviation nearly one order compared to the typically used summation method, and then achieve more accurate scan-WMS gas sensing, which can be applied in a variety of harsh environment.

RWR characterization can affect the results of WMS measurement directly. In this work, we extend the RWR-characterization model proposed by Du *et al.* and perform a more accurate RWR-characterization model with higher coupling terms to describe more coupling effects, which is referred to as the modified-three-step (M-Thr) method. We take the scanned-WMS-$2f/1f$ signals using the RWR characterized by the M-three-steps method as reference. Then, in Section 3, we analyze how the inaccuracy of the summation (Sum) and three-step (Thr) methods affects the scanned-WMS-$2f/1f$ fitted results for different modulation indexes, scan indexes, gas concentrations, and pressures. In Section 4, the experiment results show good consistency with the regular patterns in the simulation section. The modified-three-step method presents an improved accuracy in RWR description with at least 5% smaller fitting residual for all conditions compared with the three-step method, although the deviation of the deduced CO_2 concentrations between these two methods does not exceed 0.2%.

2. Experimental setup and description of the theory

2.1. Experiment setup

Figure 1 shows the experimental setup used to measure gas-parameters via the scanned-WMS-$2f/1f$ method. The function generator (Keysight 33500B) produced a sinusoidal waveform that contained a scan frequency f_s composition and modulation frequency f_m terms. A laser controller (Thorlabs ITC4001) received the superimposed signal from a function generator and sent it to a typical distributed-feedback (DFB) tunable diode laser (NEL) centered at 1432 nm, which was used to probe the CO_2 absorption transition at 6976.2026 cm^{-1}. The laser from the fiber output side was split into two parts. One part passed through a gas cell, while the other part was sent to a Fabry–Perot etalon (Thorlabs SA20012B) to determine the laser- wavelength response. The etalon had a free spectral range (FSR) of 0.05 cm^{-1}. Before the experiment, the gas cell was pumped by a pump, syringed three times, and finally filled with pure CO_2 gas to target pressure. Two parameters of the laser, the transmitted intensity and etalon signal, were probed using a photodetector (Thorlabs PDA50B2) respectively. Furthermore, the current signals, which corresponded to the two light paths, should also be recorded synchronously to serve as synchronization reference for data processing.

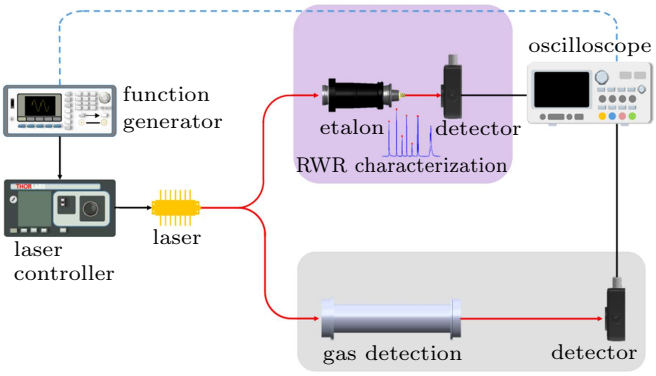


Fig. 1. Experimental system.

2.2. Relative wavelength-response characterization

There are many methods to characterize the RWR as we discussed in Section 1. The three-step method[30] shows excellent performance because it uses the fact that the amplitude of the first wavelength modulation term is proportional to the bias current. However, as we have seen in many studies, the most commonly used method for RWR characterization is the summation shown below, which is essentially the same as that

of Refs. [19–21,28,29,31] but formally adjusted here:

$$\begin{aligned} v(t) &= v_{\mathrm{c},0} + v_{\mathrm{s},1}\cdot \bar{i}_{\mathrm{s}} \sin(\omega_{\mathrm{s}} t + \phi_{\mathrm{s},1} + \eta_{\mathrm{s},1}) \\ &\quad + v_{\mathrm{s},2}\cdot \bar{i}_{\mathrm{s}}^2 \sin(2\omega_{\mathrm{s}} t + \phi_{\mathrm{s},1} + \eta_{\mathrm{s},2}) \\ &\quad + v_{\mathrm{m},1}\cdot \bar{i}_{\mathrm{m}} \sin(\omega_{\mathrm{m}} t + \phi_{\mathrm{m},1} + \eta_{\mathrm{m},1}) \\ &\quad + v_{\mathrm{m},2}\cdot \bar{i}_{\mathrm{m}}^2 \sin(2\omega_{\mathrm{m}} t + \phi_{\mathrm{m},1} + \eta_{\mathrm{m},2}), \end{aligned} \tag{1}$$

$$\begin{aligned} v(t) &= v_{\mathrm{c},0} + v_{\mathrm{s},1}\cdot \bar{i}_{\mathrm{s}} \sin(\omega_{\mathrm{s}} t + \phi_{\mathrm{s},1} + \eta_{\mathrm{s},1}) \\ &\quad + v_{\mathrm{s},2}\cdot \bar{i}_{\mathrm{s}}^2 \sin(2\omega_{\mathrm{s}} t + \phi_{\mathrm{s},1} + \eta_{\mathrm{s},2}) \\ &\quad + \left[v_{\mathrm{m},1}^{a}\cdot i_{\mathrm{s}} + v_{\mathrm{m},1}^{b}\right] \\ &\quad \times \bar{i}_{\mathrm{m}} \sin\left(\omega_{\mathrm{m}} t + \phi_{\mathrm{m},1} + \eta_{\mathrm{m},1}^{a}\cdot i_{\mathrm{s}} + \eta_{\mathrm{m},1}^{b}\right) \\ &\quad + \left[v_{\mathrm{m},2}^{a}\cdot i_{\mathrm{s}} + v_{\mathrm{m},2}^{b}\right]\cdot \bar{i}_{\mathrm{m}}^2 \sin(2\omega_{\mathrm{m}} t + \phi_{\mathrm{m},1} + \eta_{\mathrm{m},2}). \end{aligned} \tag{2}$$

Here $\omega_{\mathrm{s}} = 2\pi f_{\mathrm{s}}$, and $\omega_{\mathrm{m}} = 2\pi f_{\mathrm{m}}$. The synchronous current signal is

$$i(t) = i_{\mathrm{s}}(t) + \bar{i}_{\mathrm{m}}(t) = i_0 + \bar{i}_{\mathrm{s}}(t) + \bar{i}_{\mathrm{m}}(t), \tag{3}$$

where $i_{\mathrm{s}}(t)$ and $i_{\mathrm{m}}(t)$ are the components of the injected current scan and modulation. Here and in the following text, the subscripts (s and m) represent the laser scan and modulation terms, respectively. ϕ and φ are the initial phases of the current and beam intensity, respectively. i_0 and $\bar{i}$ are the preset center bias current and user-defined amplitude, respectively. f is the user-specified frequency. Compared to Eq. (1), the modified-three-step method (M-three-step), Eq. (2), introduces higher coupling-terms that improve the accuracy significantly. Although many variables in Eqs. (1) and (2) are represented by the same letters, they have a slight difference in values. In fact, Du *et al.* provided a description for the RWR characterization that considered the coupling term of the first modulation amplitude, which is called the three-step method (three-step) and has a worse accuracy than Eq. (2) but it is more concise.[30]

Figure 2 shows the fitted results and residuals of measured etalon peaks using summation, three-step, and the M-three-step methods. This was done with the experimental setup described in Subsection 2.1. The scan frequency and modulation frequency were $f_{\mathrm{s}} = 20$ Hz and $f_{\mathrm{m}} = 4$ kHz, respectively. When applying the summation method to fit the etalon peaks, the residual contains the obvious beat structure. From the zoomed part of Fig. 2, it can be seen that the result of the summation method is almost the same as that of the three-step or M-three-step methods at the center bias current. However, when the scan bias current deviates from the center bias current, the accuracy of the summation method decreases. Therefore, the summation method shows the largest deviation at the peaks and valleys of the scan current (see Fig. 2). This indicates that the summation method is not complete. The three-step method considers the linear relation between the coefficient of the first modulation term, which minimizes the residuals (see Fig. 2). In addition, the M-three-step method is more accurate than the three-step method, especially at the peaks and valleys of the scan current. The residuals of using the three-step method and M-three-step method are over one order of magnitude smaller than that in the summation method. Additionally, we have applied these three methods to characterize the RWR under different conditions with different DFB lasers, and the observed regular patterns were similar.

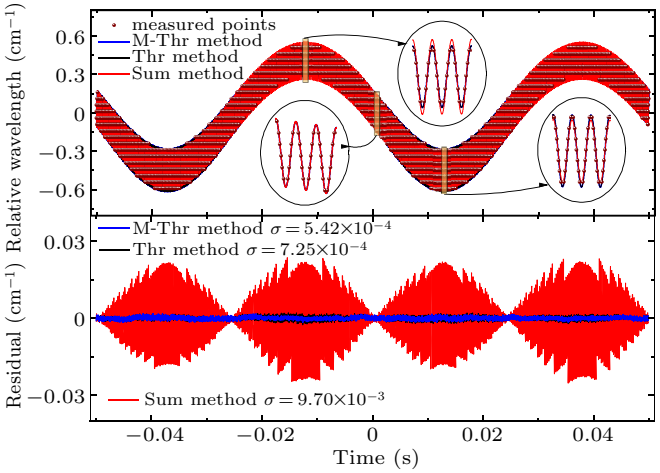


Fig. 2. Comparison of the fitting results of the summation method, three-step method, M-three-step method and their residuals.

Although Eq. (2) describes the RWR most accurately, it needs to characterize six parameters, which is laborious. Fortunately, the difference between the three-step method and M-three-step method is not large, and the former has only two parameters to characterize, which is more convenient. Even though the summation method describes the RWR worst among these methods, it is more widely used because of its convenience and simplicity in practical measurements.[28–30]

2.3. Scanned-WMS-$2f/1f$ fitting algorithm

The scanned-WMS-$2f/1f$ fitting algorithm, which was proposed and validated by Sun *et al.*[28] in 2013, requires an accurate RWR characterization. We used it as an indicator to evaluate the accuracy of the different RWR characterization methods. Here is a brief introduction of this algorithm.

Scanned-WMS-$2f/1f$ signals can be calculated as following:

$$2f/1f = \sqrt{\left[\left(\frac{X_{2f}}{R_{1f}}\right)_{\mathrm{raw}} - \left(\frac{X_{2f}}{R_{1f}}\right)_{\mathrm{bg}}\right]^2 + \left[\left(\frac{Y_{2f}}{R_{1f}}\right)_{\mathrm{raw}} - \left(\frac{Y_{2f}}{R_{1f}}\right)_{\mathrm{bg}}\right]^2}. \tag{4}$$

where the subscripts raw and bg mean raw WMS signals and background signals.

$$\begin{cases} X_{1f}(\nu) = \dfrac{G\bar{I}_0}{2}\left[H_1 + i_0\left(H_0 + \dfrac{H_2}{2}\right)\cos\psi_1 + \dfrac{i_2}{2}(H_1+H_3)\cos\psi_2\right], \\ Y_{1f}(\nu) = -\dfrac{G\bar{I}_0}{2}\left[i_0\left(H_0 - \dfrac{H_2}{2}\right)\sin\psi_1 + \dfrac{i_2}{2}(H_1-H_3)\sin\psi_2\right]. \end{cases} \tag{5}$$

where $\bar{I}_0$ is the average laser intensity, G is the electro-optical gain of the detection system, i_0 and i_2 are the amplitudes of the linear and the first nonlinear modulation terms (normalized by average laser intensity), H_k is the k^{th} harmonics of transmittance. R_{1f} refers to the root-sum-square magnitude of the X and Y components of the lock-in output in $1f$, $R_{1f} = \sqrt{X_{1f}^2 + Y_{1f}^2}$. The X_{2f} and Y_{2f} are two orthogonal components of the second order harmonics of the transmitted laser intensity, and they are obtained by multiplying the detector signal with reference signal $\cos(2\omega_{\text{m}}t)$ or $\sin(2\omega_{\text{m}}t)$ and calculate by

$$\begin{cases} X_{2f}(\nu) = \dfrac{G\bar{I}_0}{2}\left[H_2 + \dfrac{i_0}{2}(H_1+H_3)\cos\psi_1 + i_2\left(H_0 + \dfrac{H_4}{2}\right)\cos\psi_2\right], \\ Y_{2f}(\nu) = -\dfrac{G\bar{I}_0}{2}\left[\dfrac{i_0}{2}(H_1-H_3)\sin\psi_1 + i_2\left(H_0 - \dfrac{H_2}{2}\right)\sin\psi_2\right]. \end{cases} \tag{6}$$

Generally, the H_k is a function of temperature, pressure, modulation depth, and relative wavelength. However, under a certain experiment, H_k is a function of relative wavelength only, which emphasizes the necessity of obtaining accurate RWR descriptions. Sun *et al.* provided more detailed description about WMS-$2f/1f$ fitting algorithm.[28]

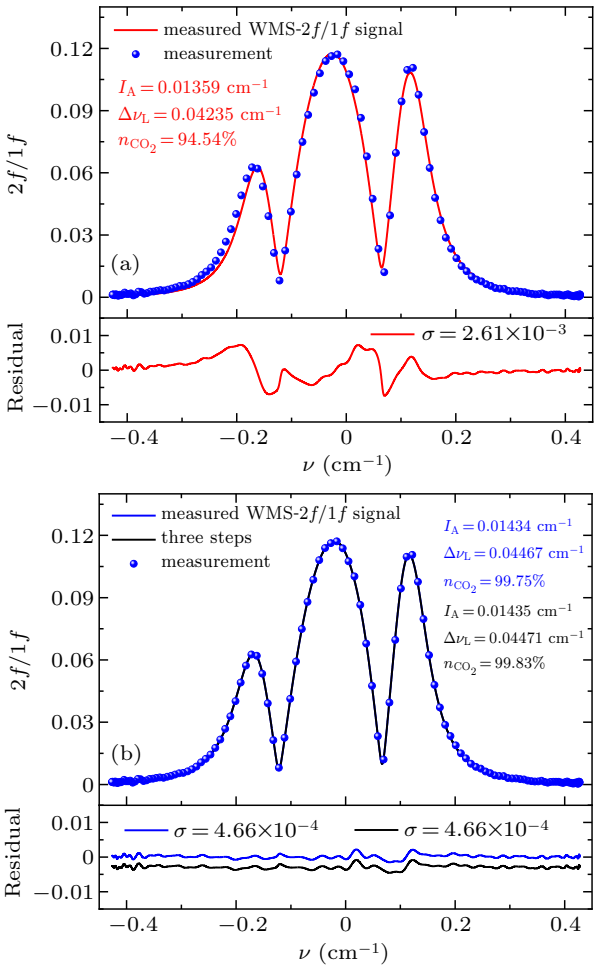


Fig. 3. A typical experiment results of WMS-$2f/1f$ fitting algorithm under 40.16 kPa, 297.5 K, and pure CO_2. The corresponding RWR characterization is shown in Fig. 2.

Figure 3 compares the measured scanned-WMS-$2f/1f$ signal with the best-fitted results of different RWR methods. The STD of the summation method is 2.61×10^{-3}, which is almost five times larger than that of the other two methods. In addition, the relative error for the concentration obtained using the three-step method or M-three-step method is about 0.2%. This number is much smaller than the 5.5% obtained for the summation method. Figure 3 indicates that the inaccuracy of the RWR characterization can induce errors for the scanned-WMS-$2f/1f$ measurement. These errors are quite large and can be efficiently minimized by providing more accurate RWR characterization models.

3. Simulation analysis

The accurate RWR characterization is extremely important for the WMS measurement. In this section, we use the summation method, three-step method, and M-three-step method with the scanned-WMS-$2f/1f$ fitting algorithm to analyze how the inaccuracy of the RWR characterization affects the scanned-WMS-$2f/1f$ fitted results. We take the scanned-WMS-$2f/1f$ signals, which were generated using the M-three-step method, as the fitting target signal. Furthermore, the variation of the scanned-WMS-$2f/1f$ fitting residuals and corresponding gas parameter deviations as a function of two laser-parameters (modulation index, scan index) and two gas-properties (concentration, pressure) was analyzed in this section. We selected an absorption transition of CO_2 and Table 1 shows the spectroscopy parameters for the CO_2 absorption transition at 6976.2026 cm^{-1}, which is adopted from Ref. [30] and HITRAN database.[32] In this section, all characteristic parameters of the laser itself were obtained by calibrating in order to be close to the real-life situation.

Table 1. Absorption spectroscopy parameters used in simulation.

ν_0 (cm^{-1})	S (cm^{-2}·atm^{-1})	γ_{air} (cm^{-1}·atm^{-1})	γ_{self} (cm^{-1}·atm^{-1})	E'' (cm^{-1})	n_{air}
6976.2026	6.987×10^{-4}	0.0872	0.1132	7.8043	0.76

3.1. Laser parameters

3.1.1. Analysis of the modulation index

The modulation index is one of the key parameters that affect the detection accuracy and sensitivity in the scanned-WMS-$2f/1f$ measurement. Changing this parameter can change not only the peak value of the scanned-WMS-$2f/1f$ signals but also the positions of two side peaks. In practical measurements, the modulation index is affected by the gas properties (concentration, temperature, pressure, etc.) and the performance of the experimental setup (laser properties, free spectral range of the etalon, etc.). Additionally, the modulation index may change with time during a dynamic measurement. Therefore, researchers always attempt to obtain the optimal modulation index, in order to improve the measurement accuracy and sensitivity. However, many studies have not considered the effects caused by the inaccuracy of the RWR description on the WMS measurement results, when the optimal modulation index is chosen.

Therefore, an analysis of how scanned-WMS-$2f/1f$ fitting residuals and corresponding relative errors vary with modulation indexes, when the summation method or three-step method is used to characterize the RWR, was performed. The simulation conditions were pure CO_2 with a pressure of 50 kPa at room temperature (297.5 K). The scan index, defined as scan depth divided by the half-width-half-maximum (HWHM), is 6, and the modulation index ranges from 0.1 to 5. The simulation results are shown in Fig. 4. The SNR is defined as the maximum value of the scanned-WMS-$2f/1f$ signal divided by the corresponding fitting residual.

Figure 4(a) shows the simulation results under different modulation indexes. The black dotted line shows the maximum values of scanned-WMS-$2f/1f$ under different modulation indexes. It increases first and then decreases with the modulation indexes. The maximum peak value is reached when the modulation index is about 1.1, which is consistent with Ref. [33]. Figures 4(b) and 4(c) show the relative error contours of WMS-$2f/1f$ fitted results, which are defined as the absolute errors normalized by the maximum value of the scanned-WMS-$2f/1f$ signal at the corresponding modulation index. In Fig. 4(b), the RWR is characterized by the summation method. It shows that the relative fitting errors are distributed in the line-center lobe and on both sides, where the $2f/1f$ values change rapidly, and they increase with increasing modulation index. In addition, we can see that the relative residual is still significant enough if the modulation index is 2.2 (see the bottom section of Fig. 4(b)). This indicates that the inaccuracy of the summation method can significantly affect the scanned-WMS-$2f/1f$ fitted results within the range of modulation indexes commonly used. Although this effect is comparatively small and the SNR, defined as the maximum peak value of scanned-WMS-$2f/1f$ divided by corresponding fitting STD, is higher when the modulation index is small, the modulation index cannot be too small to ensure sufficient signal strength and enough etalon peaks. However, in Fig. 4(c), the relative errors are almost 2 orders smaller than those in Fig. 4(b), which indicates that the three-step method is more accurate than the summation method. And the distribution is almost the same as that in Fig. 4(b). Relative fitting errors are increasing as the modulation indexes increase but the maximum value in Fig. 4(c) is only 0.13%.

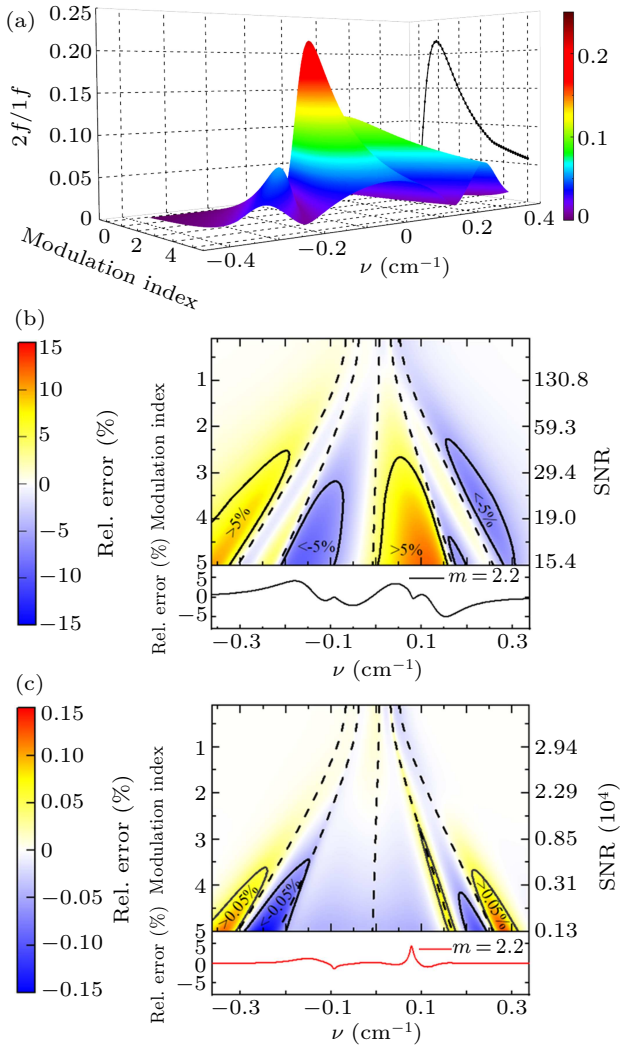


Fig. 4. (a) The simulation results of $2f/1f$ signals in different modulation indexes using the RWR characterized by M-three-step method and the maximum values of WMS-$2f/1f$ under different modulation indexes; (b), (c) the relative fitting error contours in different modulation indexes using the RWR characterized by the summation method and three-step method, respectively. In the top part, black dashed lines represent equal relative error bars and the corresponding values are ±5% in (b) and ±0.05% in (c). The bottom part shows the relative error structures at modulation index of 2.2.

Although it is hard to prove the trend shown in Fig. 4, it is still possible to obtain a qualitative explanation from Fig. 5. With the modulation index increasing, the scanned-WMS-$2f/1f$ signals extend and the RWR residuals between the M-three-step method and the summation method increase. The effective area of the scanned-WMS-$2f/1f$ signal is also mainly in the position of the larger RWR deviation (see Fig. 5). Although the SNR is decreasing, the parameter fitting residuals, using the three-step method, change very little.

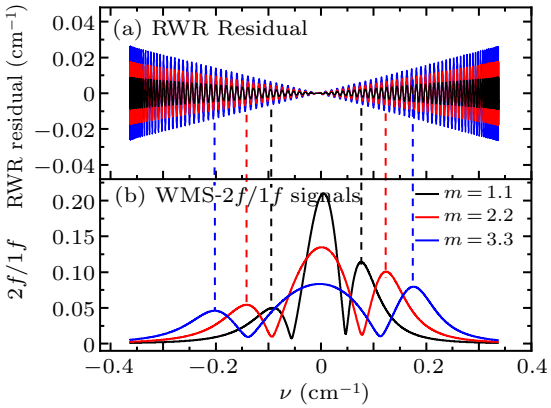


Fig. 5. (a) The corresponding RWR residuals between the M-three-step method and summation method. (b) The scanned-WMS-$2f/1f$ signals at three different modulation indexes. The dashed lines are used to indicate the peaks on both sides of scanned-WMS-$2f/1f$ signals.

Figure 6 shows the concentration and collisional broadenings fitted results and residuals for different modulation indexes, which were obtained using the scanned-WMS-$2f/1f$ fitting algorithm shown in the figure. The parameter fit residuals of the three-step method are either very small or invisible. For the fitted parameter of the summation method, the relative errors increase significantly. For small modulation indexes (< 0.5), the residuals increase slowly, with modulation indexes shown as solid lines. The maximum values are 10.5% and 12.5% for concentration and collisional broadening at the modulation index of 5. Additionally, the growth rate of the residuals, obtained using the summation method, also increases with increasing modulation indexes.

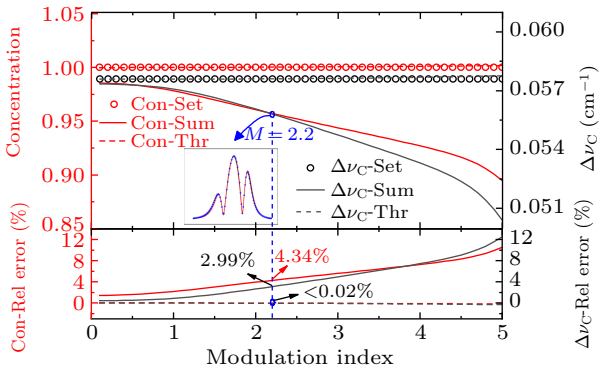


Fig. 6. Concentration and collisional broadenings obtained by fitting scan-WMS-$2f/1f$ and their residuals under different modulation indexes.

However, the results in Fig. 4 were simulated for a specific experimental condition, without considering some other effects of the real measurement. In fact, the modulation index cannot be chosen arbitrarily, instead, researchers need to consider gas properties, signal strength, and experiment apparatus performance as stated earlier. For example, the FSR of the etalon is a crucial factor in choosing the modulation index, and it cannot be too small because there would not be enough interference peaks per modulation period. Furthermore, for low-pressure conditions, where line broadening is quite narrow, the modulation index should be as small as possible under the premise of ensuring sufficient etalon peaks per modulation period and signal strength minimize the residual for fitting scanned-WMS-$2f/1f$ or gas properties caused by inaccuracy of the summation or three-step methods. For the latter, however, described using Eq. (5) in Ref. [30], the residual is still much smaller than that using the summation method to characterize RWR, especially in a large modulation index condition.

3.1.2. Analysis of the scan index

In practical measurements, the scan index is also a crucial parameter. The absorption transition cannot be scanned completely if the scan depth is too small. On the contrary, the frequency spectrum will overlap seriously if the scan depth is too large.[34] Like the modulation index, researchers should consider experimental setups, data processing, and detect objects comprehensively to obtain the optimal value of the scan index. In this subsection, the analysis of how scanned-WMS-$2f/1f$ fitting residuals and corresponding relative errors of fitted results vary with scan indexes using either the summation or three-step method to characterize RWR signals is demonstrated. The pressure and temperature are set as 50 kPa with pure CO_2 and 297.5 K, which are the same as described in Subsection 3.1.1. The scan indexes range from 4 to 10, considering the separation of the frequency spectrum. Since the amplitude of the first modulation term is not a specific value but related to the scan current, the modulation index is set to 2.2 at the center bias current.

Figure 7(a) shows the scanned-WMS-$2f/1f$ signals for different scan indexes. As can be seen, the peak values and scanned-WMS-$2f/1f$ shapes are nearly constant as the scan indexes change, only the wings become wider. Because the variation of the scan index is caused by the changes of scan current amplitude, the other parameters, such as modulation current, remain constant in this subsection.

Figures 7(b) and 7(c) are the relative error contours of scanned-WMS-$2f/1f$ fitted results, using the summation method and three-step method to characterize RWR, respectively. The variation of scan indexes hardly affects the position of the main relative errors, and the values increase slightly.

In Fig. 7(b), the maximum relative error is −5.3%, when the scan index is 10. However, it is about 2 orders of magnitude smaller in Fig. 7(c), and the maximum value in Fig. 7(c) is only 0.068%. The SNR increases with scan indexes when using the summation method shown in Fig. 7(b). However, SNR increases first and then decreases with the scan index when using the three-step method shown in Fig. 7(c).

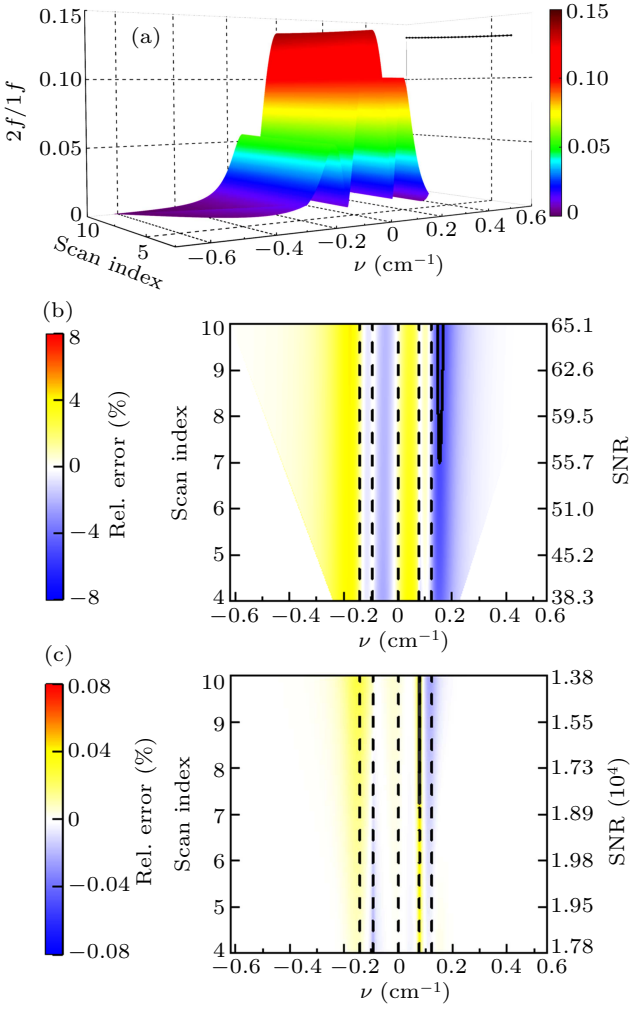


Fig. 7. (a) The simulation results of $2f/1f$ signals in different scan indexes using the RWR characterized by M-three-step method and the maximum values of scanned-WMS-$2f/1f$, (b) and (c) The fitting relative error contours in different scan indexes using the RWR characterized by summation method and three-step method, respectively, black solid lines represent equal relative-error bars, and the corresponding values are ±5% in (b) and ±0.05% in (c), the black dashed lines represent the peaks and valleys of scanned-WMS-$2f/1f$ signals for different scan indexes.

Figure 8 shows the fitted concentrations and collisional broadenings and corresponding residuals for different scan indexes. The concentration and collisional broadening fitted results for the summation method are smaller than the set values yet increase with the scan indexes. It seems as if the fitted parameters are more accurate for large scan indexes. However, we cannot draw this conclusion because the range of scan indexes used here is limited. The maximum relative errors, using the summation method (solid line in Fig. 8), are 5.27% and 3.81% for concentration and collisional broadening, respectively. The results when using the three-step method are still about 2 orders of magnitude smaller compared to using the summation method. In addition, the modulation index used here is 2.2, which can cause inherent fitting errors as analyzed in the last subsection and this indicates the importance of characterizing RWR accurately. Compared to Fig. 6, the variation of relative errors in Fig. 7 changes less than that in Fig. 6.

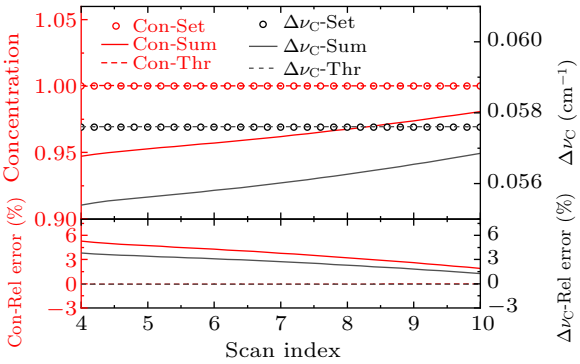


Fig. 8. Concentration and collisional broadenings obtained by fitting scan-WMS-$2f/1f$ and their residuals under different scan indexes.

The phenomena above can also be explained qualitatively. The increase of the scan index is achieved by increasing the amplitude of the scan current, such that the differences between the three methods increase with the scan index. In addition, the inaccuracies of Eq. (1) increase but the proportion of the absorbance area within a scan period is decreasing. As a result, the deviation of the parameters, between fitting and set values, decreases slightly within the scan index region under the combined effects of these two factors.

3.2. Gas properties

3.2.1. Analysis of the pressure

The gas pressure is also important in TDLAS measurements. The difference between the three methods of RWR characterization increases if the scan index and modulation index are kept constant while the pressure increases. In this section, analysis of how scanned-WMS-$2f/1f$ fitting residuals and corresponding relative errors of fitting results vary with gas pressures using summation and three-step method to characterize RWR is demonstrated. The concentration and temperature are 0.05 and 297.5 K. The scan index and modulation index are 6 and 2.2, respectively. The pressures range from 5 kPa to 100 kPa.

Figures 9(a) and 9(b) show the relative error contours of the scanned-WMS-$2f/1f$ fitted results using the summation and three-step methods to characterize RWR, respectively. Attention should be paid to the abscissa, which is defined as the relative wavenumber divided by the corresponding line broadening.

As shown in Fig. 9, the relative fitting errors increase with increasing pressure. Furthermore, the main error areas are on

both sides of the inflection points of the scan-WMS-$2f/1f$ signals, which deviate from the simulation value by more than 5%. In addition, the distribution of the relative fitting error is approximately symmetrical about the center of scan-WMS-$2f/1f$ signals but the numerical signs are opposite. Because the peak values of $2f/1f$ decrease with increasing pressure, while fitting residuals increase with increasing pressure, so that SNR decreases. Figures 9(c) and 9(d) show the fitted results. The solid lines, which represent the fitted results using the summation method, indicate that the relative errors of concentrations and collisional broadening increase rapidly with the pressure increasing. The maximum values can reach 5.5% and 4.5%, respectively.

The relative error in most of the areas in Fig. 9(b), using the three-step method to characterize RWR, is between -0.01% and 0.01%. This value is about 2 orders of magnitude smaller than that of Fig. 9(a). Only on the right of the scanned-WMS-$2f/1f$ signals, the relative error increases significantly, when the pressures are relatively large. However, the maximum never exceeds 0.1%. Although the SNR in Fig. 9(b) decreases significantly with increasing pressure, it can be seen from the red and black dashed lines in Fig. 9(c) that the relative parameter fitting error hardly changes, and the maximum relative errors are no more than 0.1%. Therefore, the relative wavelength signal, characterized by the three-step method, is accurate enough in fitting scanned-WMS-$2f/1f$ signals when the pressure varies.

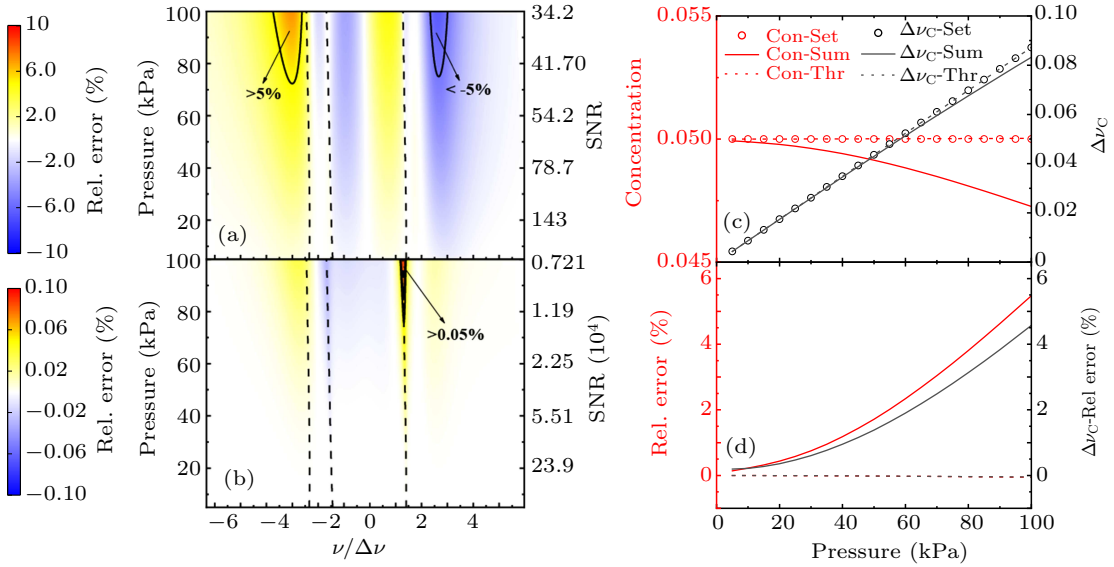


Fig. 9. (a) and (b) The relative error contours of the fitted results for different gas pressures, using the relative wavelength signals characterized by the summation method and the three-step method, respectively. The black solid line represents equal relative error bars, and the corresponding values are $\pm5\%$ in (a) and $\pm0.05\%$ in (b). The black dashed lines represent the peaks and valleys of scanned-WMS-$2f/1f$ signals for different gas pressures. (c) and (d) The fitted concentrations and collisional broadenings, and corresponding residuals.

Figure 10 gives an intuitive explanation for the above analysis. The increase in pressure results in the increase of the line widths. Therefore, both scan current and modulation current should increase to keep the scan index and modulation index constant. This can make the difference between the summation method and the M-three-step method more significant, which is shown in Fig. 10(a). As a result, the parameter fitting error increases with pressure increasing. While at low pressure, such as 20 kPa, the scanned-WMS-$2f/1f$ signal is quite narrow, and the RWR residual is relatively small. With the pressure increasing, the RWR residuals increase, and the scanned-WMS-$2f/1f$ signals extend apparently. These two factors are the main reasons for the phenomena shown in Fig. 10. In addition, the relative error of the fitted parameter is relatively small, when the gas pressure is relatively low. As shown by the dashed lines in Fig. 10(d), it is below 1%, when the pressure is lower than 35 kPa using the summation method.

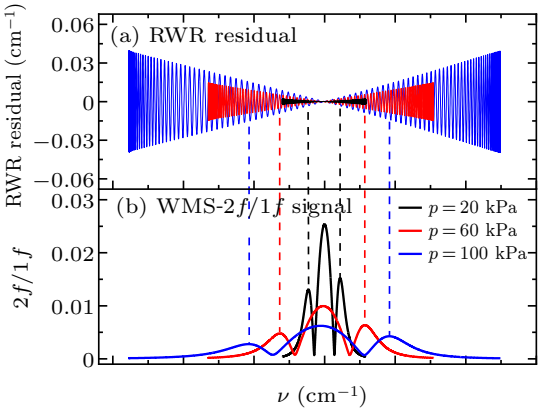


Fig. 10. (a) The corresponding RWR residuals between the M-three-step method and the summation method. (b) The scanned-WMS-$2f/1f$ signals for three different pressures. The dashed lines are used to indicate the peaks on both sides of the scanned-WMS-$2f/1f$ signals.

In fact, the scan depth or modulation depth cannot continuously decrease with decreasing pressure if certain effects in practical measurement are considered. For example, the

scan depth or modulation depth should be several times the etalon FSR to describe a scan period or modulation period precisely. When the pressure is high, the error caused by the inaccuracy of the relative wavelength characterization may be the main contributor to the measurement error. Comparatively, the three-step method can provide a more accurate description of the RWR for high gas pressures while the summation method is reluctantly acceptable if the gas pressure is relatively low. It should be noted that the mole fraction used here is 0.05, which could cause a large error if the mole fraction is larger.

3.2.2. Concentration analysis

Accurate measurement of the gas concentration is a main goal of TDLAS detection. However, if the characterization of the RWR is not accurate enough, the benefits of WMS, which are gained by using a more complicated data process, are weakened. Nevertheless, many previous studies did not take this effect into account. In this subsection, we analyze how scanned-WMS-$2f/1f$ fitting residuals and corresponding relative errors of fitted results vary with gas concentration, using either the summation or three-step method to characterize RWR. The pressure and temperature are 50 kPa and 297.5 K, respectively. The scan index and modulation index are 6 and 2.2, respectively. The CO_2 mole fraction ranges from 0.01 to 1.

Figures 11(a) and 11(b) are the relative error contours of scanned-WMS-$2f/1f$ fitted results using summation method and three-step method to characterize RWR, respectively. The abscissa is defined as the relative wavenumber divided by the corresponding collisional broadening. Although the peak of the scanned-WMS-$2f/1f$ increases with gas concentration, the relative errors stay almost constant and the contour lines are nearly straight lines. This means that the deviation of scanned-WMS-$2f/1f$, caused by the inaccuracy of the RWR characterization, always exists and does not depend on the gas concentration variation. The main error area in Fig. 11(a) is located on both sides of the three peak positions, and the maximum relative error is -4.86%, where the concentration is 1. For the same areas in Fig. 11(b), the errors are approximately 2 orders of magnitude smaller than that in Fig. 11(a), and only a small part of the area exceeds 0.01%. Also, the maximum value in Fig. 11(b) is 0.043%, indicating that the three-step method is accurate enough to characterize RWR in WMS measurements, and the accuracy is hardly affected by the gas concentration variation.

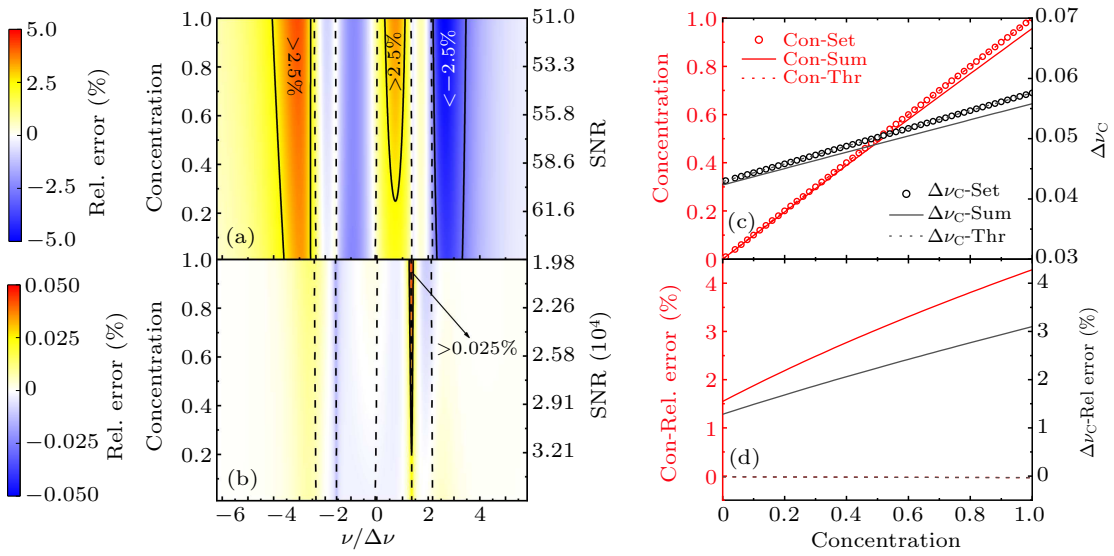


Fig. 11. (a) and (b) The fitting relative error contours in different gas concentrations using the relative wavelength signals characterized by summation method and three-step method, respectively; the black solid line represents equal relative error bars, and the corresponding values are $\pm 2.5\%$ in (a) and $\pm 0.025\%$ in (b). The black dashed lines represent the peaks and valleys of scanned-WMS-$2f/1f$ signals in different gas concentrations. (c) and (d) The concentration and collisional broadenings obtained by fitting scanned-WMS-$2f/1f$ and their relative errors.

Figure 11(c) shows the gas concentrations and collisional broadenings obtained by fitting scanned-WMS-$2f/1f$ signals in different gas concentrations. Figure 11(d) shows the corresponding relative errors. The results, when using the summation method, vary significantly, and the relative errors increase from 1.55% to 4.28% for the concentration and from 1.28% to 3.10% for collisional broadening as concentrations increase. On the other hand, the relative errors, which are caused by the inaccuracy of the three-step method, are almost negligible.

These trends are due to the increase in concentration and the following effects. The primary effect is that the absorption increases in the areas where the RWR description by the summation method deviates substantially from the real RWR with increasing gas concentration. On the other hand, the increase in CO_2 concentration causes a larger HWHM, which also increases the proportion of absorption in the areas with larger deviation from the RWR characterization.

According to the analysis above, the effect due to the inaccuracy of the RWR characterization at low concentration also causes more than 1% error using the summation method.

This may be the major error in the practical measurement if the concentration is relatively large. Furthermore, if the etalon FSR is much larger than that in this section, the fitting error will become more significant. In general, parameter fitting errors, using RWR characterized by the three-step method, are always much smaller and less affected by the gas concentrations.

4. Analysis of the experiment

As discussed in the simulation analysis section, the scanned-WMS-$2f/1f$ and gas parameters fitting relative errors are relatively less sensitive to scan index or gas concentration variation while compared to modulation indexes or pressures. The difference between summation method and three-step method or M-three-step method is within 2% if the modulation index is less than 0.5 or within 1% if the gas pressure is less than 35 kPa, but has large difference under large modulation index or high gas pressure conditions. Therefore, we focus on the experimental results for different modulation indexes and gas pressures. The experiment setup and process were introduced in Subsection 2.1.

4.1. Different modulation indexes

Figure 12 demonstrates the measured scanned-WMS-$2f/1f$ signals and fitting residuals when using the three different RWR characterization methods for $m = 1.39$ and $m = 3.82$ on the right, while the corresponding RWR characterizations are shown on the left. The deduced concentrations are also shown in the figure. Considering that the relative errors of the fitting collisional broadening are almost the same as that of fitting concentrations, we do not show them here.

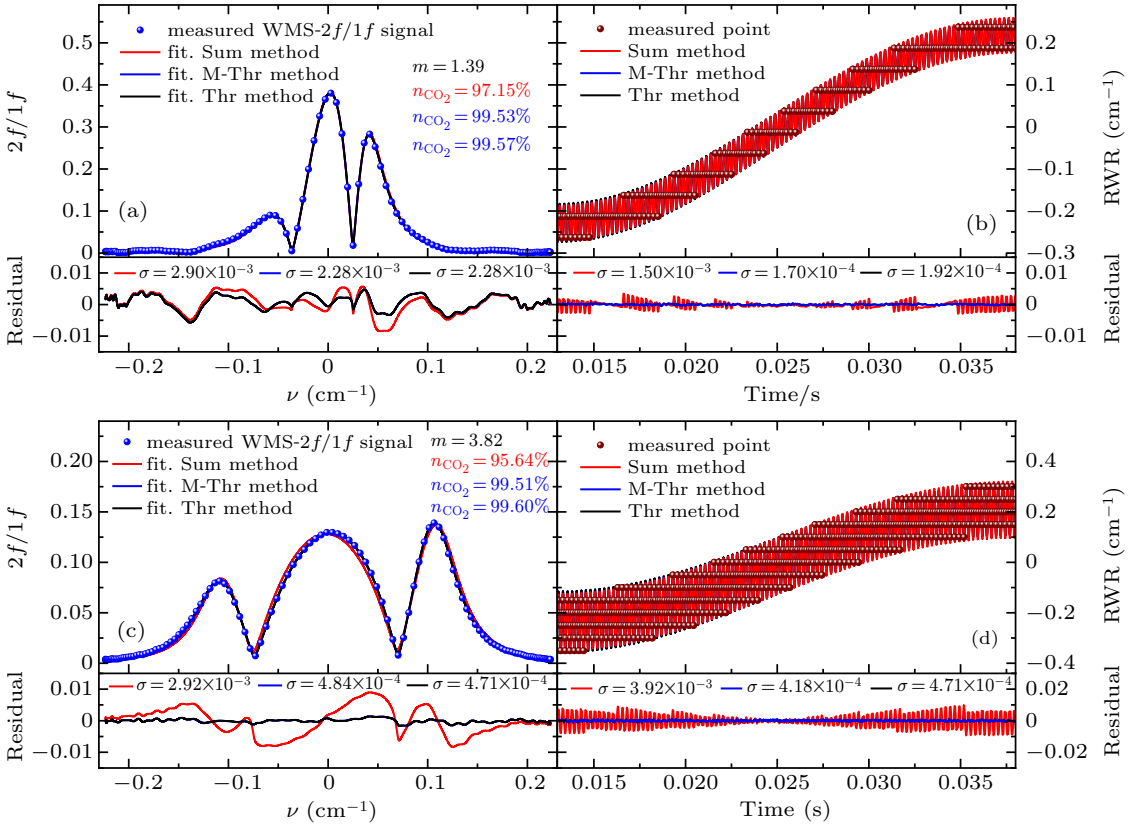


Fig. 12. (a) and (c) The scanned-WMS-$2f/1f$ fitted results for $m = 1.39$ and 3.82, respectively. (b) and (c) The corresponding RWR characterizations. The scan index is about 7.5 for both (a) and (c). The measurements were conducted with temperature and pressure of 298.1 K and 25.18 kPa, and an optical length of 52.5 cm.

As we can see, the scanned-WMS-$2f/1f$ fitting residuals, obtained using the summation method, show obvious features around the center lobes, which can be minimized by applying the three-step method or M-three-step method, especially in the large modulation index. In Fig. 12(a), the modulation index is about 1.39, and the deduced concentrations are 97.15%, 99.57%, and 99.53% with the summation method, three-step method, and M-three-step method, respectively. The relative errors are smaller compared to the ones shown in Fig. 6 for the same modulation index, which may be due to the lower pressure and larger scan index used here. When the modulation index is 3.82, shown in Fig. 12(c), the relative errors of concentration obtained by using three-step or M-three-step method still do not exceed 0.5%. However, they can rise to 4.36% for the summation method, which indicates that the three-step method and the M-three-step method can still work efficiently to obtain accurate parameter through fitting scanned-WMS-$2f/1f$ signals under large modulation indexes while the inaccuracy of the summation method has caused large deterioration of gas parameter fitted results. This

is consistent with the simulation analysis above. When the modulation index is 1.39, the fitting standard deviations of all the three methods are quite large. This may be due to the larger value of the scanned-WMS-$2f/1f$.

4.2. Different gas pressures

Figure 13 shows the measured scanned-WMS-$2f/1f$ signals and fitting residuals for the three different RWR characterization methods for gas pressures of 19.63 kPa and 59.55 kPa. The corresponding RWR characterizations are shown in the figure.

For 19.63 kPa gas pressure, shown in Fig. 13(a), the concentration deviations are only 0.34% and 0.42% when using the three-step and M-three-step methods. However, it becomes 2.88% when using the summation method. For 59.55 kPa gas pressure, shown in Fig. 13(c), the performance of the summation method is worse, and the deviation reaches 6.29%, while the deviations for the three-step and M-three-step methods are still quite small (0.40% and 0.56%) and within the uncertainty of the gas concentration and the spectroscopy parameters.[30] The deviations of the deduced concentration by the summation method are significant, both at low and high gas pressure. However, three-step and M-three-step methods can still deliver accurate results under high modulation conditions. It should be noted that the concentration deviation obtained by the summation method is larger than that in Sunsection 3.2.1 under identical pressures, which may be caused by the higher concentration of CO_2 used in these experiments.

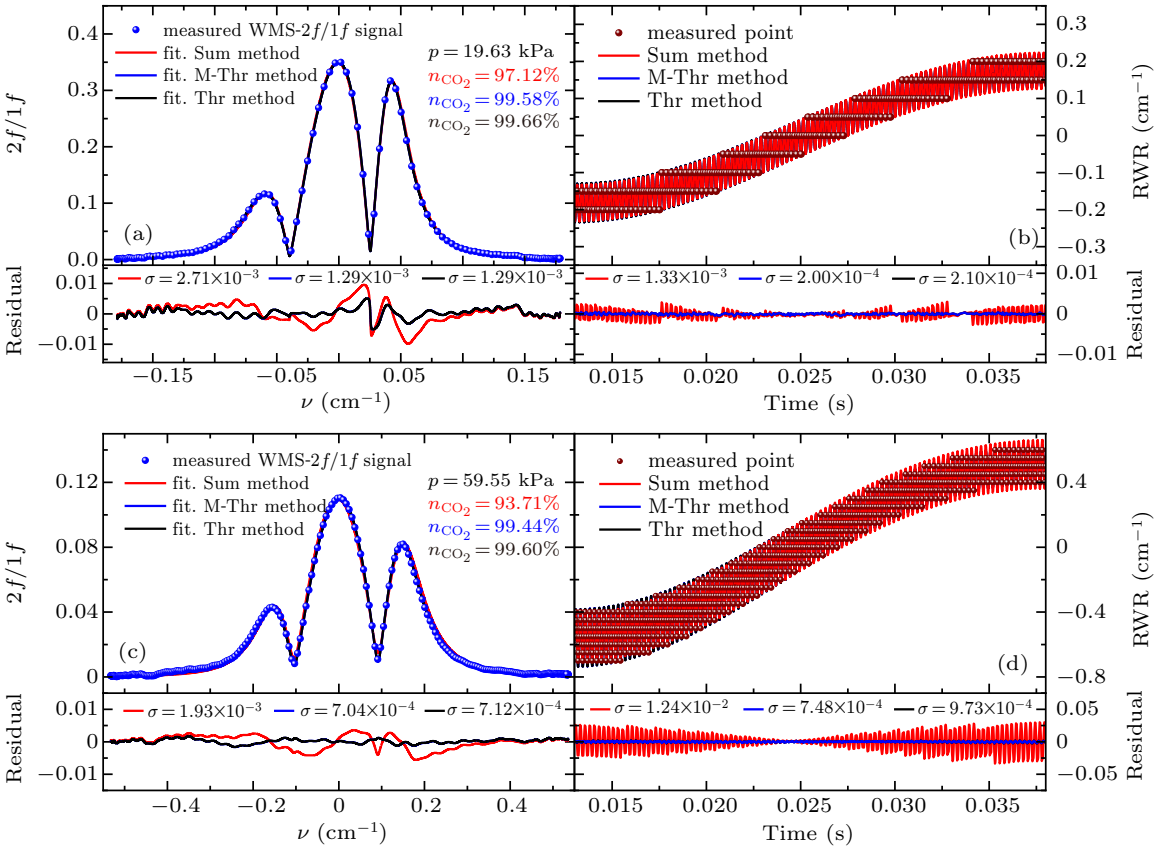


Fig. 13. (a) and (c) The scanned-WMS-$2f/1f$ fitting results under pressures of 19.63 kPa and 59.55 kPa, respectively. (b) and (d) The corresponding RWR characterization results. The scan index and modulation index are about 7.5 and 2.1 at the center current. The room temperature is 299.3 K and the absorption path length is 52.5 cm.

5. Conclusion

In this paper, a more accurate RWR characterization method is proposed based on the high order coupling terms between laser scan and modulation. The performance of three RWR characterization methods in scanned-WMS gas sensing is compared under different modulation indexes, scan indexes, gas concentrations, and gas pressures. The three-step method, which considers the first coupling term, can significantly improve the scanned-WMS $2f/1f$ fitting accuracy. The M-three-step method has a higher RWR characterization accuracy than the three-step method, but the difference between these two methods, in terms of parameter fitting errors, do not exceed 0.2%. Therefore, the three-step method is still recommended for scanned-WMS gas sensing from the application point of view. The summation method, which has been used most commonly, is reluctantly acceptable under small modulation indexes or low gas-pressures, where the deduced parameter errors are relatively small but still larger than those of the three-step or M-three-step methods.

The simulation results indicate that the relative fitting errors are less sensitive to the scan index and gas concentration but greatly affected by the modulation index and gas pressure

when using the summation method to characterize RWR. The concentration fitting error, which is caused by the inaccuracy of the summation method, is relatively small for a small modulation index (below 2% if $m < 0.5$) or low gas pressure condition (below 1% if $p < 35$ kPa). However, it can rise to 10% or 4% under the large modulation index ($m = 5.0$) or high gas pressure ($p = 100$ kPa). Even if the modulation index is 2.2, the relative error can still reach 3%. The relative fitting errors of the three-step method or M-three-step method are 2 to 3 orders of magnitude smaller than that of the summation method, which suggests the high accuracy of the three-step or M-three-step method for RWR characterization.

To further validate the above-mentioned conclusions from the simulation analysis, the CO_2 absorption transition at 6976.2026 cm^{-1} was measured by scanned WMS with different modulation indexes and gas pressures. The STD of the fitting RWR using the summation method is about one order higher than that of three-step or M-three-step method in all experiments. Similarly, because of the inaccuracy of the summation method RWR signal, the STD of fitting scanned-WMS-$2f/1f$ signal is also larger, especially under $m = 3.82$ or $p = 59.55$ kPa condition. And the corresponding deduced relative errors of the gas concentrations are near 2.88% under $m = 1.39$ or p = 19.63 kPa. They even increase to 4.36% or 6.29% under $m = 3.82$ or $p = 59.55$ kPa. On the other hand, the deduced relative errors of the concentration of using three-step or M-three-step methods are both within 0.6%. The experimental results are in good agreement with the trends found in the simulation analysis.

References

[1] Hanson R K 2015 CLEO: 2015 STh4O.1
[2] Shao J Xiang J D, Axner O and Ying C F 2016 *Appl. Opt.* **55** 2339
[3] Zhang Z Pang T, Yang Y, Xia H, Cui X, Sun P, Wu B, Wang Y, Sigrist M W and Dong F 2016 *Opt. Express* **24** A943
[4] Li J D Peng Z M and Ding Y J 2020 *Optics and Lasers in Engineering* **126** 105875
[5] Pogány A Klein A and Ebert V 2015 *J. Quant. Spectrosc. Radiat. Transfer* **165** 108
[6] Girard J J Choudhary R and Hanson R K 2018 *J. Quant. Spectrosc. Radiat. Transfer* **221** 194
[7] Du Y J Peng Z M and Ding Y J 2018 *Opt. Express* **26** 9263
[8] Campbell M F Wang S K, Goldenstein C S, Spearrin R M, Tulgestke A M, Zaczek L T, Davidson D F and Hanson R K 2015 *Proceedings of the Combustion Institute* **35** 231
[9] Laich A R Ninnemann E, Sneha N, Ramees R, Samuel B, Pitz W J, Goldsborough S S and Vasu S S 2020 *Combust. Flame* **212** 486
[10] Johnson S E Davidson D F and Hanson R K 2020 *Combust. Flame* **216** 161
[11] He D, Peng Z M and Ding Y J 2019 *Combust. Flame* **207** 222
[12] Amato F D and Rosa M D 2002 *Optics and Lasers in Engineering* **37** 533
[13] Li H J, Farooq A, Jeffries J B and and Hanson R K 2008 *J. Quant. Spectrosc. Radiat. Transfer* **109** 132
[14] Goldenstein C S and Hanson R K 2015 *J. Quant. Spectrosc. Radiat. Transfer* **152** 127
[15] Peng Z M, Du Y J and and Ding Y J 2020 *Sensors (Basel)* **20** 681
[16] Peng Z, Du Y and Ding Y 2020 *Sensors (Basel)* **20** 616
[17] Cui R Y, Dong L, Wu H P, Li S Z, Zhang L, Ma W G, Yin W B, Xiao L T, Jia S T and Tittel F K 2018 *Opt. Express* **26** 24318
[18] Tommasi E D, Casa G and Gianfrani L 2006 *Appl. Phys. B* **85** 257
[19] Li H J, Rieker G B, Liu X, Jeffries J B and Hanson R K 2006 *Appl. Opt.* **45** 1052
[20] Sun K, Chao X, Sur R, Jeffries J B and Hanson R K 2012 *Appl. Phys. B* **110** 497
[21] Wei W, Peng W Y, Wang Y, Choudhary R, Wang S K, Shao J K and Hanson R K 2018 *Appl. Phys. B* **125** 9
[22] Kluczynski P, Jahjah M, N?hle L, Axner O, Belahsene S, Fischer M, Koeth J, Rouillard Y, Westberg J, Vicet A and Lundqvist S 2011 *Appl. Phys. B* **105** 427
[23] Qu Z C Ghorbani, R, Valiev D and Schmidt F M 2015 *Opt. Express* **23** 16492
[24] Chen J, Hangauer A, Strzoda R and Amann M C 2010 *Appl. Phys. B* **102** 381
[25] Liu J X, Zhou, Y T, Guo S J, Hou J J, Zhao G, Ma W G, Dong L Wu Y Q, Zhang L, Yin W B, Xiao L T, Axner O and Jia S T 2019 *Opt. Express* **27** 1249
[26] Zhao G Tan W, Hou J J, Qiu X D, Ma W G, Li Z X, Dong L, Zhang L, Yin W B, Xiao L T, Axner O and Jia S T 2016 *Opt. Express* **24** 1723
[27] Sur Ritobrata, Peng W Y, Strand Christopher, Spearrin M R, Jeffries J B, Hanson R K, Bekal Anish, Halder Purbasha, Poonacha S P, Vartak Sameer and Sridharan Arun K 2017 *J. Quant. Spectrosc. Radiat. Transfer* **187** 364
[28] Sun K, Chao X, Sur R, Goldenstein C S, Jeffries J B and Hanson R K 2013 *Meas. Sci. Technol.* **24** 125203
[29] Goldenstein C S Strand C L, Schultz I A, Sun K, Jeffries J B and Hanson R K 2014 *Appl. Opt.* **53** 356
[30] Du Y J Peng M Z and Ding Y J 2020 *Opt. Express* **28** 3482
[31] Kluczynski P and Axner O 1999 *Appl. Opt.* **38** 5803
[32] Gamache R R and Lamouroux J L 2013 *J. Quant. Spectrosc. Radiat. Transfer* **130** 158
[33] Peng W Y, Strand C L and Hanson R K 2019 *Appl. Phys. B* **126** 17
[34] Rieker G B, Jeffries J B and Hanson R K 2009 **48** 5546